Mon. Not. R. Astron. Soc. **274,** 861–868 (1995)

A search for primordial anisotropies in the cosmic microwave background radiation: first observations at 13.5 GHz with the Cosmic Anisotropy Telescope

Créidhe O'Sullivan, G. Yassin, G. Woan, P. F. Scott, Richard Saunders, M. Robson, Guy Pooley, A. N. Lasenby, S. Kenderdine, Michael Jones, M. P. Hobson and P. J. Duffett-Smith

Mullard Radio Astronomy Observatory, Cavendish Laboratory, Madingley Road, Cambridge CB3 0HE

Accepted 1995 January 10. Received 1995 January 9; in original form 1994 November 21

ABSTRACT

We report the first observations of the cosmic microwave background radiation (CMBR) at 13.5 GHz made with the Cosmic Anisotropy Telescope (CAT) near Cambridge. After removal of foreground radio sources brighter than 10 mJy, using the Ryle Telescope (RT), the map shows evidence for residual structure on a scale of approximately 1/2° with an rms variation of 18 mJy. We intend to use multifrequency measurements to distinguish between Galactic and CMBR components.

Key words: instrumentation: interferometers – cosmic microwave background – cosmology: observations.

1 INTRODUCTION

Temperature anisotropies in the cosmic microwave background radiation are expected to result from inhomogeneity in the matter distribution at the surface of last scattering. Measurements of these primordial anisotropies provide powerful constraints on theories of structure formation in the early Universe. Observations on different angular scales probe the amplitude of structures on different mass scales.

On angular scales $> 3°$, the Sachs–Wolfe effect (Sachs & Wolfe 1967) is expected to be a principal cause of anisotropy, and the *COBE* satellite has already detected anisotropies at a level of $(\Delta T/T)_{\rm rms} = 1.1 \times 10^{-5}$ on an angular scale of about 10° (Smoot et al. 1992). Many current experiments are sensitive to degree scales, with both detections and upper limits similar to that of *COBE* (see, e.g., Schuster et al. 1993; Gundersen et al. 1993; Cheng et al. 1994; Ganga et al. 1993). There have also been attempts to detect anisotropies on arcmin scales (e.g. Subrahmanyan et al. 1993; Fomalont et al. 1993; Myers, Readhead & Lawrence 1993). For a review of recent experiments, see Lasenby & Hancock (1994). On angular scales between 10 and 60 arcmin, Doppler scattering is expected to dominate and may indeed produce a value of $\Delta T/T$ greater than at any other scale. The CAT has been designed especially to detect primordial anisotropies in the range 10–60 arcmin.

The CAT (Robson et al. 1993) is a three-element interferometer which can operate at any frequency between 13 and 17 GHz, with an observing bandwidth of 500 MHz and a system temperature of 50 K. The system temperature is continuously measured using a modulated 1-K noise signal which is injected into each antenna. The baselines are variable from 1 to 5 m, and for these CMBR observations baselines of approximately 1.6 and 2.5 m were used, giving a synthesized beam of 25×22 arcmin^2 (FWHM). In order to remove the effects of the Galaxy, the CAT will operate between 13 and 17 GHz, with scaled configurations to give the same synthesized beam at different frequencies. The antenna primary beam has a FWHM of 2°.2 at 15 GHz. The CAT simultaneously records data from orthogonal linear polarizations. However, its alt–az mount means that the plane of polarization rotates on the sky as the telescope tracks a given field. The telescope is surrounded by a 5-m high earth bank lined with aluminium to form a ground shield. This shielding reduces the effect of spillover and terrestrial radio interference, but also limits observations to elevations greater than 25°.

Interferometers offer significant advantages for CMBR observations (Saunders 1986), and we have carried out tests to check that the CAT performance is indeed not compromised by systematic effects due to the atmosphere, crosstalk between antennas, or correlator offsets. Here we report on some aspects of the commissioning of the instrument, and its first measurements of the CMBR.

2 CAT COMMISSIONING

2.1 Preliminary maps

We begin by mapping Cassiopeia A, which is one of the brightest sources at cm wavelengths (331 Jy at 15 GHz). Its high declination makes it suitable for observation over long periods with the CAT. Fig. 1 shows a CLEANed map of the

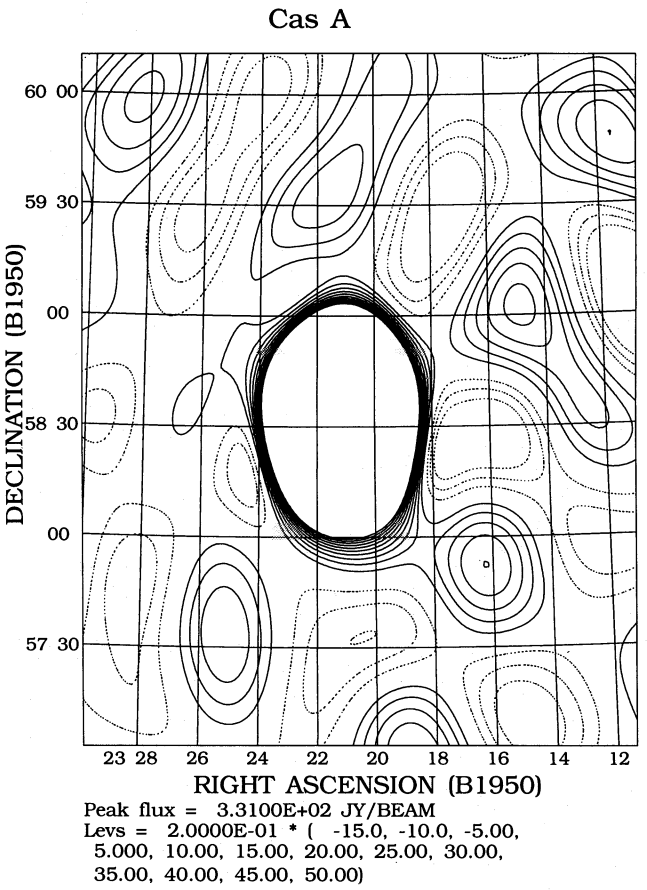

Figure 1. CLEANed map of Cas A. Contours within the central unresolved region have not been drawn.

source made from an 8-h observation at 15.5 GHz (only low flux density contours are shown). It is unresolved by the CAT so that, in the absence of any phase errors, the shape of the resulting image would be just that of the 'clean beam' (an elliptical Gaussian fitted to the central region of the dirty beam). The map is consistent with there being no phase errors greater than 5°.

Next, we mapped the radio source 0836+71, a much fainter source whose visibility amplitude and phase could not be distinguished from noise in the 0.22-s primary integration period. It has a flux density of 1 Jy at 15.5 GHz and is near the field chosen for deep CMBR observation. We made a map with the source offset by 30 arcmin from the pointing centre as shown in Fig. 2. The peak apparent flux density is 700 mJy, consistent with the reduction expected from the primary beam pattern, and the noise is as predicted given the bandwidth and measured system temperature. This test demonstrates that our data reduction and mapping procedures are correct.

From these and other observations of radio sources we have determined the rms phase uncertainty after 8 h of observation to be about 5°, so that a single observation on a bright source once per night is sufficient for calibration.

2.2 Crosstalk

Crosstalk can arise between closely spaced elements, especially at low elevations when shadowing of one element by another may occur. Radiation leakage form one horn, which is picked up by another, results in correlated output which can add systematically in places on the map. We have carried out experiments which show that at elevations above 40°, where no shadowing occurs, the cross-coupling between antennas is always less than −50 dB, and false features on maps from this cause are never brighter than 1 mJy (Robson 1994).

2.3 Correlator offsets

Any unstable offsets introduced by an interferometer's correlator can be especially serious for CMBR observations due to the large integration times and high sensitivity required. Such an offset, being largely constant in phase, shows up as a feature at the north celestial pole (NCP), since rotation of the signal phase to the pointing centre is carried out in the software after recording. Sidelobes of this feature, if it were sufficiently large, could have an appreciable effect, even on a map whose centre lay well away from the NCP. CAT incorporates phase switching to remove the d.c. offset introduced by the correlator. This offset is averaged over 10^4 measurements and subtracted. Fig. 3 shows a typical data set for five nights' observations. We find that this offset varies by less than 0.1 Jy between each 10^4-s average.

Fig. 4 shows a map, with pointing centre at RA $8^h20^m00^s$, Dec. +69°, which was made with no phase rotation applied. The map was made from about 300 h of data. An offset would appear as a feature at the centre of the map, but there is nothing in the map that is inconsistent with the expected noise level. Even if the weak feature, labelled 'A', near the map centre were in fact due entirely to an offset, its sidelobes would add artefacts no larger than 400 μJy to a map made at declination +69°, where we carried out deep CMBR observations.

All our commissioning tests have shown that the CAT is operating correctly and is capable of reaching the sensitivities required for CMBR anisotropy observations.

3 OBSERVATIONS

3.1 Choice of field

There are several factors to be considered when choosing a field for deep observations with the CAT. Most importantly, it must lie well away from regions of bright radio emission such as the Galactic plane and bright radio sources. We therefore scaled the 408-MHz all-sky radio survey of Haslam et al. (1982) to 15 GHz with a spatially variable spectral index calculated between 408 and 1420 MHz (Reich & Reich 1986), convolved the result with a 1° beam, and then looked for low brightness regions of the sky suitable for CAT observations. Fields at high declination were most suitable as they were above the CAT radiation screen for longer periods. However, we discarded fields too near the north pole where the natural fringe frequency would be too low to provide a useful distinction between wanted and unwanted signals. The Green Bank 4.85-GHz sky maps (Condon, Broderick & Seielstad 1989) were also used to locate regions of the sky relatively free from bright radio sources, a difficult task because of the large field of view of the CAT. Flux densities at 1.4, 2.7, 5 and 10.7 GHz (Kühr et

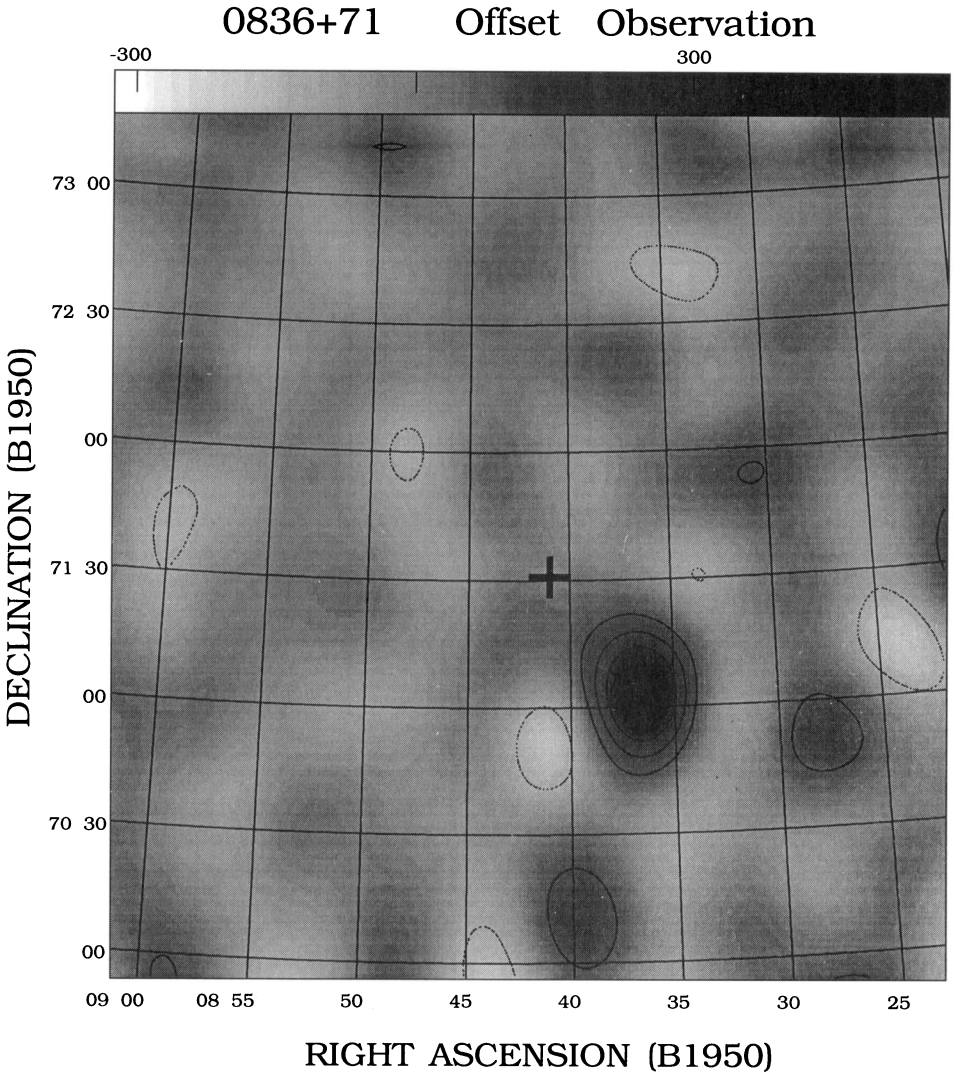

Figure 2. 8-h observation of 0836 + 71, offset by 30 arcmin. The pointing centre is at RA 8^h41^m, Dec. $+70°30'$ (B1950). The noise on the map is 60 mJy and the peak flux is 700 mJy. No correction for the primary beam has been made.

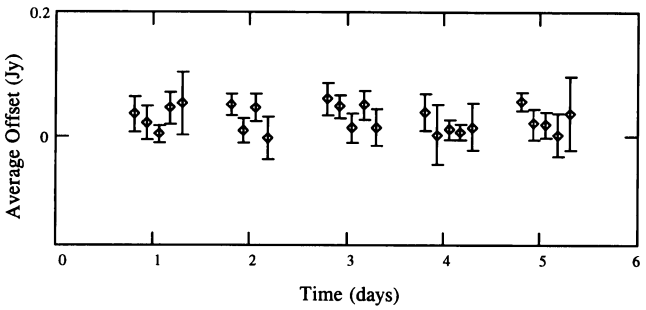

Figure 3. Correlator offset (averaged over 10^4 measurements) as a function of time.

al. 1981), where available, were used to give some estimate of the source flux densities at 15 GHz.

Each candidate field was scanned using a raster technique with the Ryle Telescope to produce a map of the central $2° \times 2°$ region with a noise level of 2 mJy and a resolution of 30 arcsec (Pooley, in preparation). Features brighter than 10 mJy (5σ) were identified as sources. Further observations of these, and other bright peripheral sources identified from the 4.85-GHz maps, were then made with the Ryle Telescope for accurate source subtraction. We identified one field (hereafter referred to as CAT1) at B1950 $\alpha = 8^h20^m00^s$, $\delta = +60°00'00''$, which contained few sources brighter than 5 mJy at 4.85 GHz within the half-power points of the primary beam, and we carried out deep observations here with the CAT over an extended period.

3.2 Observing strategy

The CAT1 field was observed for six weeks from 1993 December to 1994 February. During this period the field was above the screen for about 16 h each night. No observations were made below an elevation of 40°. The observations were made at night to avoid solar interference. Cas A was observed for 1 h at the beginning and end of each night's run for calibration purposes.

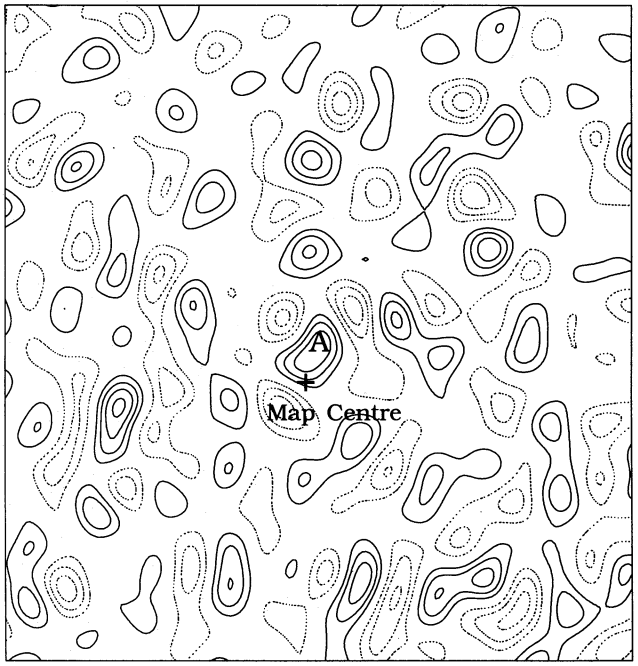

Peak flux = -3.0344E-02 JY/BEAM
Levs = 2.0000E-03 * (-15.0, -12.0, -9.00,
-6.00, -3.00, 3.000, 6.000, 9.000, 12.00,
15.00)

Figure 4. 13.5-GHz map of an 8°×8° field with no phase rotation applied. The telescope pointing centre was RA $8^h20^m00^s$, Dec. +60°. The feature marked 'A' has a flux density of 20 mJy. The noise on the map is 7 mJy.

3.3 Data reduction

The measured visibility amplitudes were first adjusted to take account of the variation in gain as a result of system temperature fluctuations. Flux and phase calibrations were then carried out using the observations of Cas A. The phases of the recorded signals were reduced in software to a common reference at the pointing centre. Calibrated data were averaged over 100 s before being converted to UVFITS format (Greisen & Harten 1981) and passed to the NRAO AIPS package for further processing. Robson et al. (1994) have already discussed the effects of weather conditions on CAT observations. We scanned each night's data by eye and discarded all sections obviously affected (using AIPS task UVFLAG). Even if the interference was only evident on the shorter spacings, data taken during the relevant time period were discarded from all baselines. As noted by Robson et al., the bad points were easy to detect and we were able to use more than 60 per cent of the data in making the final map. We also applied a 3σ clip (AIPS task UVCLIP) to minimize the effect on the final map of single-point excursions. The rms noise level of the remaining data showed no variation with baseline length, as is expected if no weather contamination remained at a significant level. Successive data files were then concatenated (AIPS task DBCON) and maps made using the AIPS task HORUS. A total of about 300 h of good data was left after editing and these were used to make the maps shown in the remainder of this paper.

4 RESULTS

4.1 Maps

Fig. 5 shows a map made when orthogonal polarizations are subtracted from one another. This cancels the unpolarized component of any astronomical signal. The polarizations of the radio sources are typically a few per cent or less and the contribution from any polarized component of the CMBR is negligible. Linearly polarized components are reduced by the rotation of the two polarizations on the sky. The rms power in the central region of the map (where any remaining astronomical signal should be a maximum), σ_n, is the same as that measured away from the map centre and is entirely consistent with the calculated instrumental noise. We measure $\sigma_n \approx 7$ mJy. This map, and those that follow, have not been corrected for the primary beam of the telescope, the half-power points of which are approximately 1° from the pointing centre. All the maps shown, with the exception of Figs 1 and 2, have been made using natural weighting.

Our noise level corresponds to an antenna temperature, T_A, of 18 μK, close to the best sensitivity achieved so far in CMBR experiments of 13.5 μK (ACME South Pole experiment of Schuster et al. 1993). The conversion between antenna temperature sensitivity and the sensitivity to brightness temperature on the sky is described by Hobson, Lasenby & Jones (1995) and is applied to the data in this paper by Scott et al. (in preparation). For an assumed Gaussian autocorrelation function on the sky, the correction factor, which accounts for the relative underfilling of our aperture as compared with a single dish, is approximately 2 (see Hobson et al. 1995). However, for the remainder of the current paper we present our results in the unambiguous units of flux density.

Fig. 6 shows the map produced when the two polarizations were added together. The noise level well away from the centre is the same as that on the previous map (σ_n), but now astronomical signals appear in that part of the map covered by the primary beam. The variance in this region of the map, σ^2, includes contributions from the instrumental noise (σ_n^2), radio sources (σ_s^2), the Galaxy (σ_{Gal}^2) and the CMBR (σ_{CMBR}^2). The variance due to radio sources can conveniently be considered as the sum of the variance due to sources with a flux density greater than 10 mJy (our RT completeness limit), $\sigma_{s>10\,mJy}^2$, and that due to sources with flux densities less than 10 mJy, σ_{conf}^2 (which give rise to confusion noise). We therefore write

$$\sigma^2 = \sigma_n^2 + \sigma_{Gal}^2 + \sigma_{CMBR}^2 + \sigma_{conf}^2 + \sigma_{S>10\,mJy}^2.$$

After correction for the primary beam pattern we find that $\sigma = 40$ mJy in the field of view of the antennas.

4.2 Point-source subtraction

The CAT does not have the range of baselines necessary to distinguish between radio sources and other signals such as the CMBR, and hence we use the RT (with its higher resolution) to perform this function. Although the CAT was designed to be sensitive to extended structure (it has small baselines), point radio sources were, in fact, the dominant contribution to the CAT1 map. The positions and 15.2-GHz flux densities of all sources brighter than 10 mJy in the central 2°×2° of the field were accurately known from the

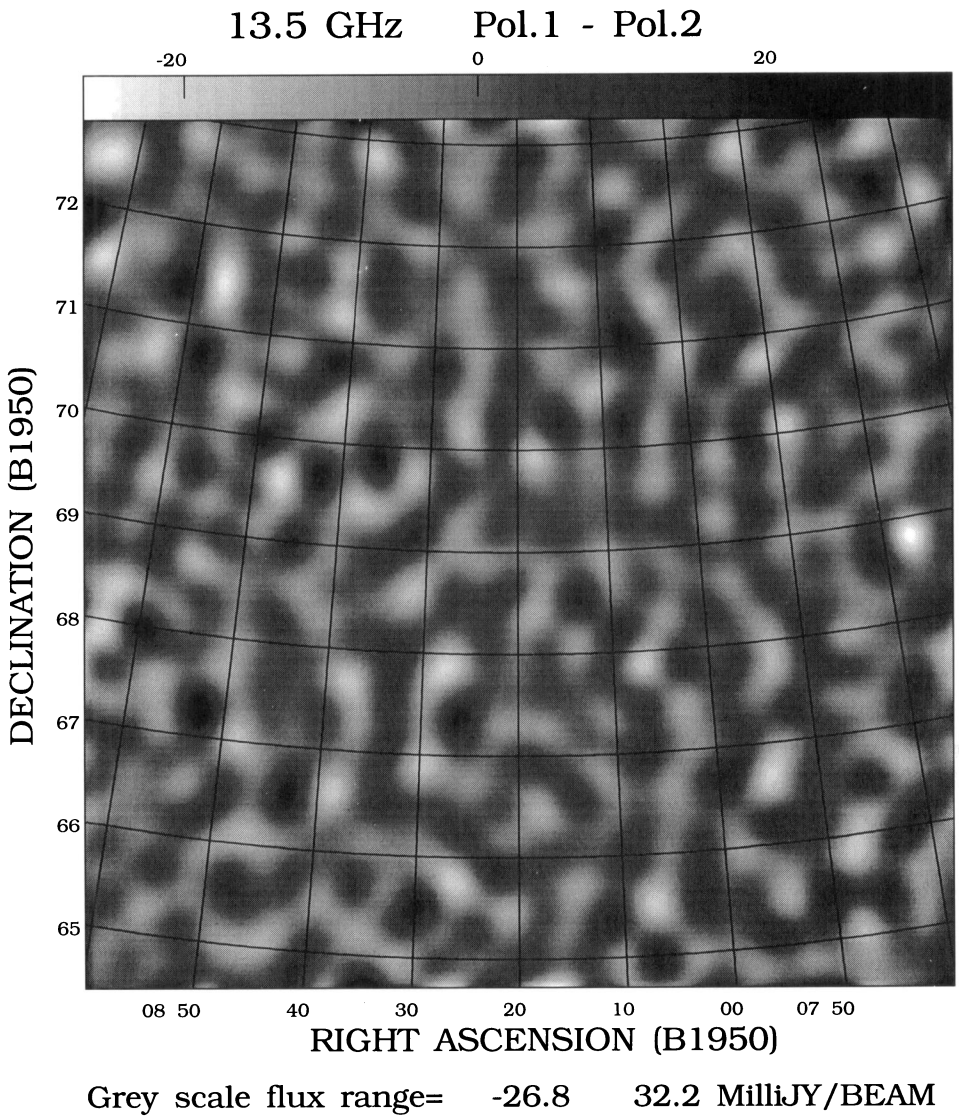

Figure 5. 13.5-GHz map of the CAT1 field showing the difference between orthogonal polarizations. The FWHM of the CAT primary beam is approximately 2°.

RT raster scans. 15 sources were subtracted from this region, with 15.2-GHz flux densities ranging from 10 to 140 mJy. The subtraction was carried out in the *uv* plane. Additional RT observations were made of all sources brighter that 15 mJy that were close enough to the map centre to contribute 10 mJy or more to the CAT1 map, and these were also subtracted. In all we subtracted the visibilities of 31 sources from the CAT visibilities.

Most sources exhibited falling spectra between 4.85 and 15.2 GHz. For these sources the 13.5-GHz flux density was calculated using linear interpolation. In one case there was clear evidence that the source had two spectral components, one whose flux density fell with frequency, superposed on another whose flux density rose with frequency; we interpolated each component separately. For those sources appearing on the RT scans but not on the 4.85-GHz map the spectrum was assumed flat.

Fig. 7 shows a simulation of the map which would have been obtained had the CAT observed these 31 sources alone on an otherwise blank sky with no instrumental noise.

The RT was also used to monitor sources for variability. Two of the sources, with 15.2-GHz fluxes of about 10–15 mJy, showed evidence for variability at about the 20 per cent level over a period of a few days. These were monitored by the RT.

4.3 Source-subtracted map

Fig. 8 shows the map made after source subtraction. Comparison with Fig. 5 shows that there is excess variance (σ_{ss}^2) towards the centre of the map, given by

$$\sigma_{ss}^2 = \sigma^2 - \sigma_{S>10\,\mathrm{mJy}}^2$$

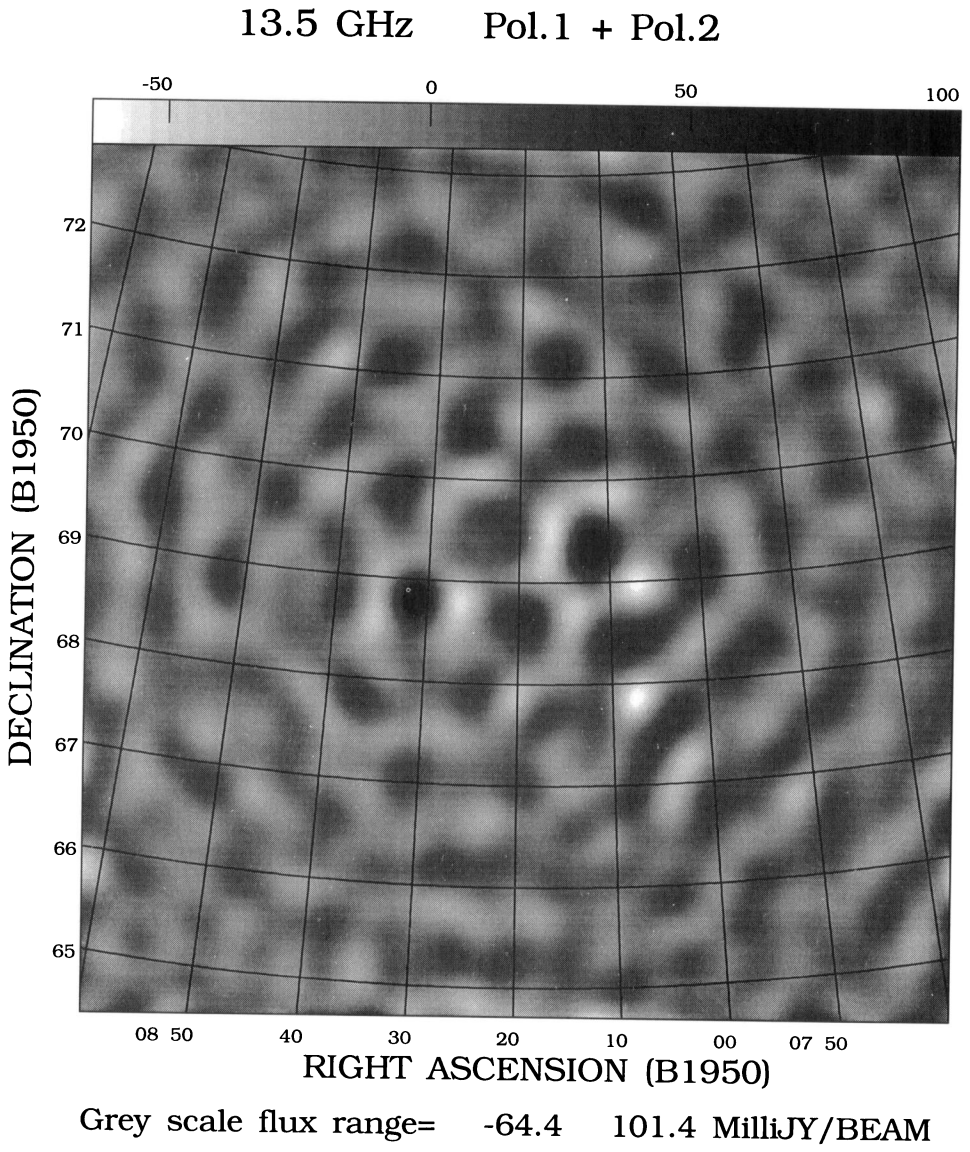

Figure 6. 13.5-GHz map of the CAT 1 field with orthogonal polarizations added.

or

$$\sigma_{ss}^2 = \sigma_n^2 + \sigma_{conf}^2 + \sigma_{CMBR}^2 + \sigma_{Gal}^2.$$

We measure $\sigma_{ss} = 20.0$ mJy.

To investigate the effect of the flux density interpolation, the spectral indices of the sources between 13.5 and 15.2 GHz were set randomly at either $+2.5$ or -2.5, and the source subtraction procedure repeated. This was done four times and gave a mean value of $\sigma_{ss} = 22 \pm 0.5$ mJy (compared with 20.0 mJy, from our best estimate of the 13.5-GHz flux densities from the 15.2-GHz and lower flux density data). As expected, the residual variance was higher, but the proximity of the CAT and RT frequencies meant that the effect of varying the spectral indices was small. It was obvious from the final source-subtracted maps if any of the brighter sources had been subtracted incorrectly.

Franceschini et al. (1989) have discussed the problem of discrete source contributions to small-scale anisotropies of the CMBR, and have shown the difficulty they present for primordial anisotropy measurements. The confusion noise due to foreground sources has been calculated by Condon (1974) as

$$\sigma_{conf}^2 = \left[\frac{\Omega K}{(3-\gamma)(\gamma-1)\ln 2}\right] S_{max}^{3-\gamma},$$

where the differential source counts obey

$$\frac{dN(s)}{dS} = KS^{\gamma}.$$

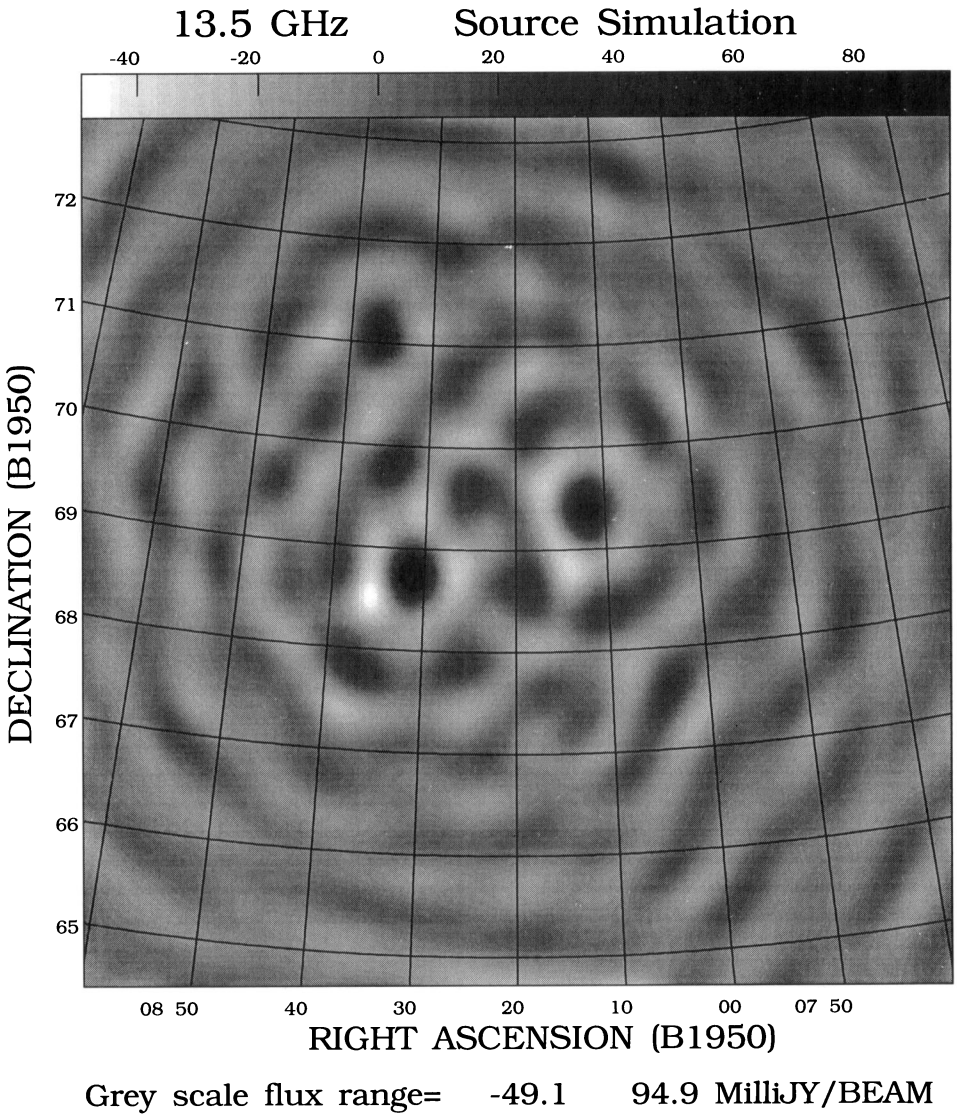

Figure 7. 13.5-GHz simulated noiseless map of the CAT 1 field containing only foreground (discrete) sources.

$N(S)$ is the number of sources in the flux interval $[S, S+\mathrm{d}S]$, Ω is the synthesized beam solid angle, and $S_{\max}$ is the largest source flux density remaining after source subtraction (10 mJy in our case). This gives $\sigma_{\mathrm{conf}} = 5$ mJy. Hence we find

$$(\sigma^2_{\mathrm{CMBR}} + \sigma^2_{\mathrm{Gal}})^{1/2} = 18 \text{ mJy}.$$

This rms is the same as that for the sky after convolution with our synthesized beam, which has an FWHM of 25×25 arcmin^2 (at PA $= -10°$) for the main positive lobe, but which has an extended negative region as well. The range of angular scales on which the CAT has sensitivity to structure on the sky may be found by a detailed statistical calculation (e.g. Hobson et al. 1995). For structures with a Gaussian-shaped covariance function with coherence angle θ_c (corresponding to the dispersion of the Gaussian), The sensitivity is within one-half of its maximum over the range $5 < \theta_c < 25$ arcmin.

This is clear evidence for residual emission at 13.5 GHz that is consistent with reported levels of primordial anisotropy, but we shall need more measurements at other frequencies within the CAT band before we can discriminate between CMBR and Galactic contributions.

5 CONCLUSIONS

Preliminary tests have shown that the CAT is reaching its design sensitivity. We find no evidence for residual effects due to correlator offset, crosstalk, gain or phase instability. During typical winter conditions 60 per cent of the data collected can be used. We have observed one candidate field (CAT 1) at 13.5 GHz, with approximately 300 h of data being used to make the final map. The Ryle Telescope has made raster scans at 15.2 GHz with sufficient sensitivity to subtract foreground radio sources, and after source subtraction the data show evidence for residual structure. Careful analysis and future measurements at other frequencies will allow us to determine the CMBR component of this anisotropy.

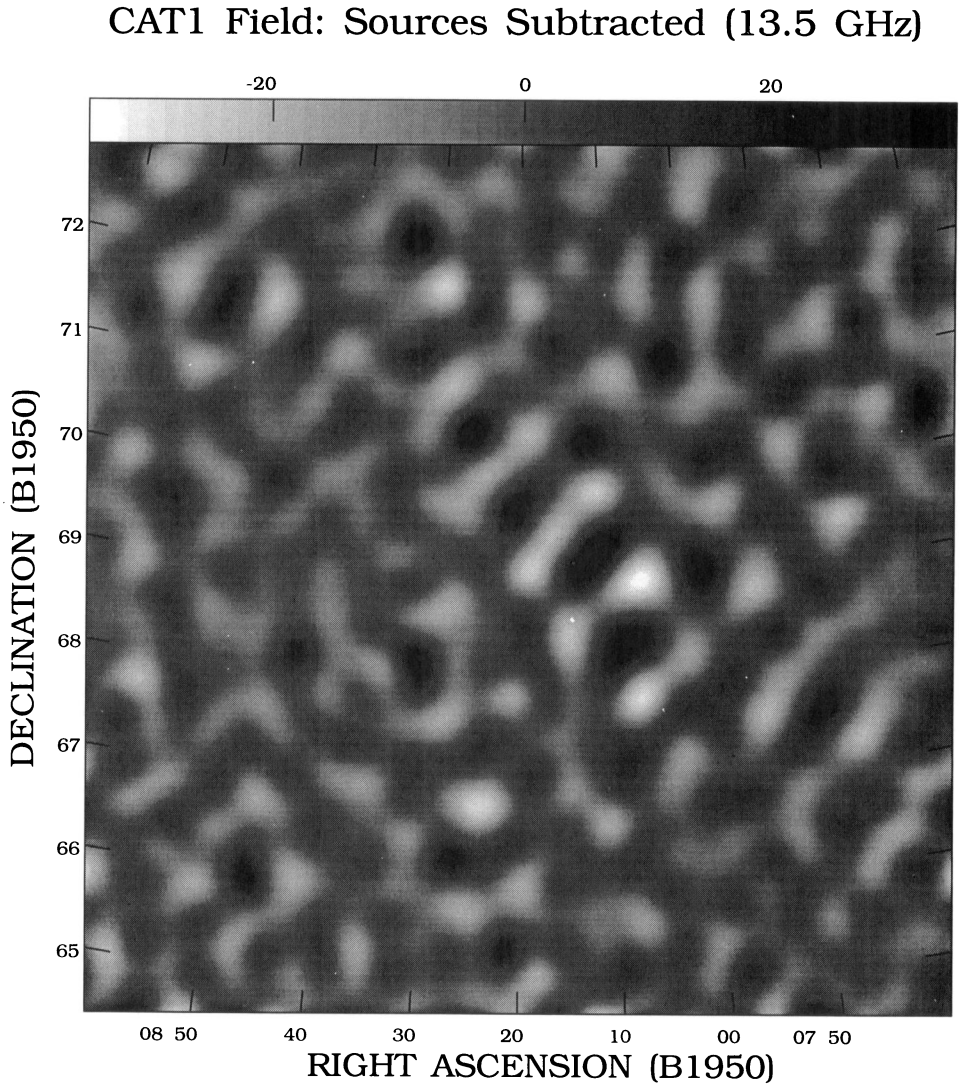

Figure 8. 13.5-GHz map of the CAT 1 field with 31 sources subtracted.

ACKNOWLEDGMENTS

We thank the staff at the Observatory for help with the CAT. CO'S acknowledges an EC Human Capital and Mobility Fellowship and a PPARC studentship. We gratefully acknowledge PPARC financial support for the CAT.

REFERENCES

Cheng E. S. et al., 1994, ApJ, 422, L37
Condon J. J., 1974, ApJ, 188, 279
Condon J. J., Broderick J. J., Seielstad G. A., 1989, AJ, 97, 1064
Fomalont E., Partridge R. B., Lowenthal J. D., Windhorst R. A., 1993, ApJ, 404, 8
Franceschini A., Toffolati L., Danese L., Der Zotti G., 1989, ApJ, 344, 35
Ganga K., Cheng E., Meyer S., Page L., 1993, ApJ, 410, L57
Greisen E. W., Harten R. H., 1981, A&AS, 44, 371
Gundersen J. O. et al., 1993, ApJ, 413, L1
Haslam C. G. T., Salter C. J., Stoffel H., Wilson W. E., 1982, A&AS, 47, 1
Hobson M. P., Lasenby A. N., Jones M., 1995, MNRAS, in press
Kühr H., Pauliny-Toth I. I. K., Witzel A., Schmidt J., 1981, AJ, 86, 854
Lasenby A. N., Hancock S., 1994, in Sato K., ed., Evolution of the Universe & its Observational Quest. Universal Academy Press, Tokyo, p. 137
Myers S. T., Readhead A. C. S., Lawrence C. R., 1993, ApJ, 405, 8
Reich P., Reich W., 1986, A&AS, 63, 205
Robson M., Yassin G., Woan G., Wilson D. M. A., Scott P. F., Lasenby A. N., Kenderdine S., Duffett-Smith P. J., 1993, A&A, 277, 314
Robson M., 1994, PhD thesis, Univ. Cambridge
Robson M., O'Sullivan C. M. M., Scott P. F., Duffett-Smith P. J., 1994, A&A, 286, 1028
Sachs R. K., Wolfe A. M., 1967, ApJ, 147, 73
Saunders R. D. E., 1986, in Swings J. P., ed., Proc. IAU Symp. Vol. VII, Highlights of Astronomy. Reidel, Dordrecht, p. 325
Schuster J., Gaier T., Gundersen J., Meinhold P., Koch T., Seifert M., Wuensche C. A., Lubin P., 1993, ApJ, 412, L47
Smoot G. F. et al., 1993, ApJ, 396, L1
Subrahmanyan R., Ekers R. D., Sinclair M., Silk J., 1993, MNRAS, 263, 416

Opposite p. 886, MNRAS, **274**

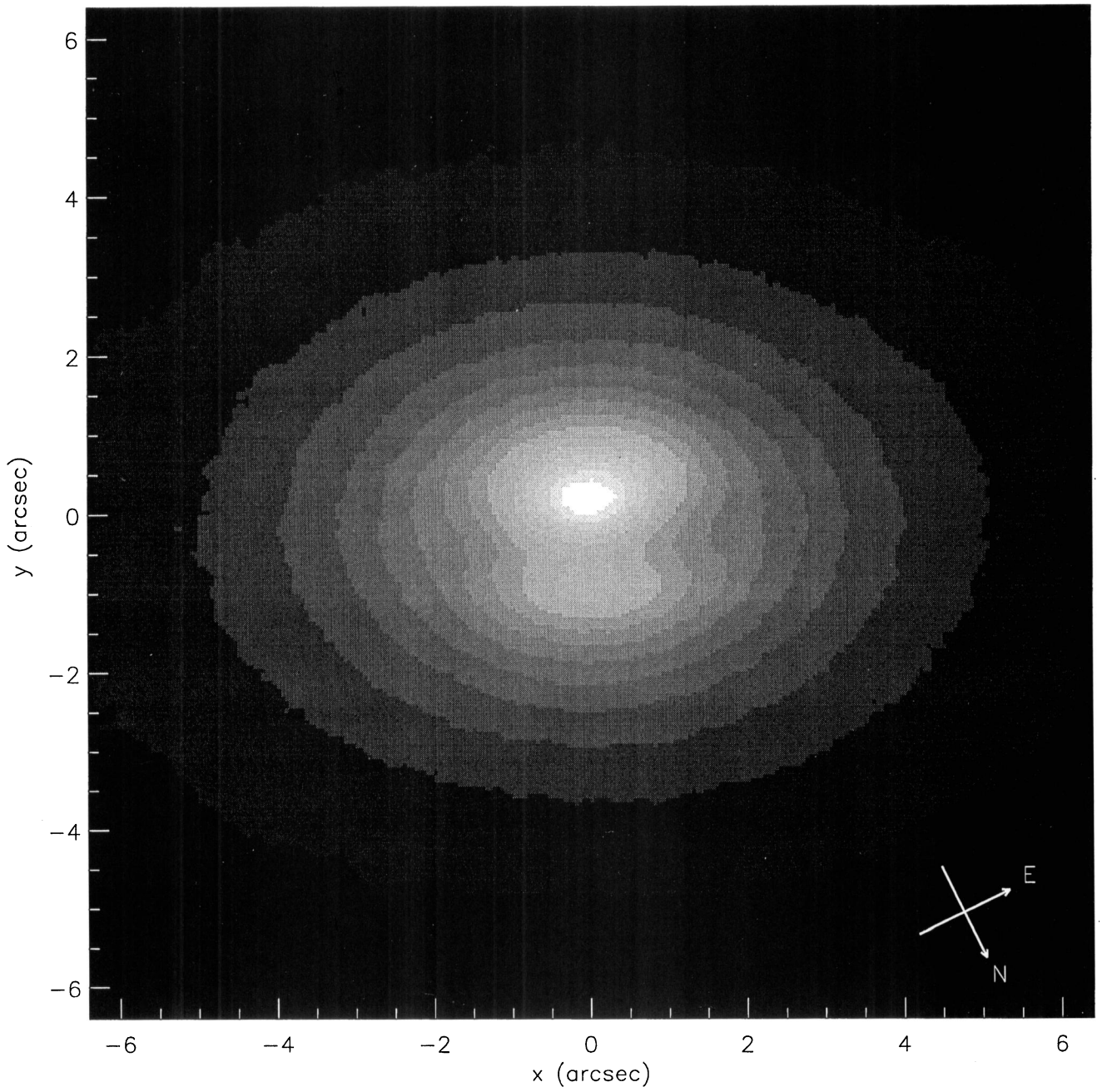

Figure 1. *R*-band image of the central region of NGC 7052, obtained with seeing FWHM $S = 0.67$ arcsec. The directions of north and east are as indicated. There is a dust lane in the inner 2 arcsec, aligned with the major axis of the galaxy.